Durability of clinker reduced shotcrete: Ca^{2+} leaching, sintering, carbonation and chloride penetration

Marlene Sakoparnig ⬡ · **Isabel Galan** · **Florian R. Steindl** · **Wolfgang Kusterle** ·
Joachim Juhart · **Cyrill Grengg** · **Lukas Briendl** · **Andreas Saxer** ·
Maria Thumann · **Florian Mittermayr**

Abstract The reduction of clinker use is mandatory to lower the negative environmental impact of concrete. In shotcrete mixes, similarly to the case of conventional concrete, the use of supplementary cementitious materials (SCMs) and proper mix design allow for the substitution of clinker without compromising the mechanical properties. However, the impact of the substitution on the durability of shotcrete needs to be further assessed and understood. The results from the present study, obtained from real-scale sprayed concrete applications, show a reduction of the Ca^{2+} leaching and sintering potential of clinker-reduced shotcrete mixes due to the presence of SCMs. This positive effect, crucial for low maintenance costs of tunnels, is mainly related to a reduced portlandite content, which on the other hand negatively affects the carbonation resistance of shotcrete. Additionally, the hydration of SCMs positively influences the chloride penetration resistance presumably due to a combination of microstructural changes and changes in the chloride binding capacity. Differences found in the pore size distribution of the various mixes have low impact on the determined durability parameters, in particular compared to the effect of inhomogeneities produced during shotcrete application.

Keywords Durability · Shotcrete · Leaching · Carbonate precipitation · Carbonation · Chloride penetration

M. Sakoparnig (✉) · J. Juhart · L. Briendl ·
F. Mittermayr
Institute of Technology and Testing of Construction
Materials, Graz University of Technology, Graz, Austria
e-mail: m.sakoparnig@tugraz.at

I. Galan · F. R. Steindl · C. Grengg
Institute of Applied Geosciences, Graz University of
Technology, Graz, Austria

W. Kusterle · M. Thumann
Concrete Laboratory, OTH Regensburg, Regensburg,
Germany

A. Saxer
Institute for Material Technology, University of
Innsbruck, Innsbruck, Austria

1 Introduction

Shotcrete is a type of concrete, which is applied on surfaces by means of a spraying (shooting) process. The application of shotcrete can be done by dry-mix or wet-mix procedure: for dry-mix shotcrete, the mixture consisting of binder and aggregates is pneumatically transported through a hose to the nozzle, where the water is added by the nozzleman. In contrast, for wet-mix shotcrete the binder is mixed with aggregates and water before it gets pumped to the nozzle, where in

most cases a setting accelerator is added [1]. Shotcrete can be sprayed in thin layers, also overhead and formwork is not needed. Therefore, shotcrete is used for many different applications like slope stabilization, swimming pools, concrete repair work [2], architectural applications [3] and, most frequently, for underground structures like tunnels [4, 5]. During the past decades shotcrete technology developed in many ways (equipment, chemical admixtures, etc.) [4]. However, to reduce the environmental impact, more research for sustainable and durable shotcrete is still required [6, 7].

The durability of all concretes is influenced by physical (porosity) and chemical (phase assemblage, pore solution) parameters. In the case of shotcrete, those parameters differ from conventional concrete due to several reasons: (1) the use of setting accelerators and special fast-setting binders leads to different hydrated phase assemblages and pore solution chemistry [8, 9], and (2) the application method influences the porosity [10, 11], the matrix homogeneity [12–15], and the binder to aggregate ratio [16–18]. The type of durability issue affecting shotcrete depends on the environmental surroundings [19]. In tunnels, primary durability problems are sulphate attack, leaching and sintering. Sulphate attack causes expansion reactions, strength loss, cracking and disintegration of the shotcrete matrix [20–24]. Concrete leaching and ion transport can lead to carbonate sintering in places like the tunnel drainage system, where blockage may occur [25, 26]. Next to the primary durability problems in tunnels, other durability issues related to steel corrosion, like carbonation and chloride diffusion, may occur if shotcrete is used in certain aggressive environments or in permanent constructions. Few studies have dealt with the durability of shotcrete [20–24, 27–33]. In particular, to the best of the authors' knowledge, no study has investigated the Ca^{2+} leaching of real-scale shotcrete samples in combination with carbonation and chloride penetration resistance.

Due to the aforementioned differences between concrete and shotcrete, not all results and knowledge from concrete can be directly transferred to shotcrete. Even studies performed on accelerated hand-mixed samples may not be used to predict the behaviour of shotcrete exposed to certain aggressive environments, since the spraying (shooting) process has a direct impact on physiochemical material properties [34]. In the present study, newly developed shotcrete mixes with reduced clinker content were sprayed in real-scale tests, cured in steady lab conditions, and analysed in terms of leaching, sintering, carbonation (accelerated vs natural) and chloride penetration performance. The influences of binder composition and the spraying process on the durability properties are discussed.

2 Background

2.1 Ca^{2+} leaching and carbonate sintering

The precipitation of carbonates can take place through different processes depending on geogenic (natural) and man-made (technical) environmental conditions [35]. The most relevant technical parameter for this study is the interaction of shotcrete with the local groundwater in underground structures. Ions (Ca^{2+}, Na^+, K^+, Sr^{2+}, OH^-, etc.) with a negative concentration gradient between the pore solution and the groundwater diffuse and discharge as highly alkaline drainage solutions. On the one hand undersaturation in the pore solution, caused by the diffusion, leads to congruent and incongruent dissolution processes such as portlandite dissolution or C–S–H decalcification, respectively [36–39]. The resulting Ca-depleted phase assemblage is often referred to as the leaching zone [38, 40, 41]. On the other hand high pH drainage solutions may precipitate massive calcium carbonate either due to the reaction of dissolved portlandite with hydrogen carbonate (Eq. 1) or due to the uptake of CO_2 from the atmosphere [26]. Further parameters such as temperature, CO_2 partial pressure, Mg^{2+} content, water mixing, microbial activity, drainage type etc., are known to greatly influence the precipitation of carbonates in tunnel drainages and therefore rates can also differ within the same tunnel site [25, 26, 35, 42].

$$Ca^{2+} + (OH)^- + HCO_3^- = CaCO_3 + H_2O \qquad (1)$$
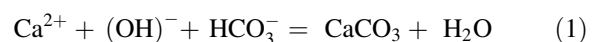
In tunnels, insulation layers are often placed between shotcrete and concrete to prevent water ingress and reduce the water pressure on the construction. The groundwater is transported by side-drains and collected in most cases in a central drainage. Clogging with $CaCO_3$ in the drainage system is

problematic for tunnel structures operation as this leads to increasing water pressure, which can ultimately even result in a failure of the structure [33, 43, 44]. Countermeasures comprise mechanical removal of the $CaCO_3$, e.g. high pressure water jetting, and/or adding chemicals such as acids, water softeners, hardness stabilizers, dispersing agents, etc. [43, 45, 46]. However, the most straightforward concept is to directly reduce the sintering potential of the shotcrete by applying state of the art shotcrete technology, as presented in this study.

2.2 Carbonation and chloride diffusion

Both carbonation and chloride diffusion can negatively affect the durability of steel-reinforced shotcrete and steel tension members or anchor heads applied in shotcrete-based geotechnical applications (e.g. for slope stabilisation). In concrete/shotcrete, steel is protected from electrochemical corrosion due to the passivation layer that forms under the highly alkaline conditions provided by the pore solution. As a result of carbonation, the high pH of the pore solution drops and the passivation layer becomes unstable [19, 47]. Locally, the layer can also be damaged by Cl^- ions through the creation of small anodes [48, 49]. The rates, at which chloride diffusion and carbonation progress, are influenced by the composition of the cement matrix and the permeability of the concrete, especially that of the interfacial zone, and are therefore often used as indicators for shotcrete quality.

2.2.1 Carbonation

The chemical reactions involved in the carbonation process are similar to those of the carbonate sintering. However, in concrete literature the term carbonation refers mainly to the precipitation processes that take place in the concrete matrix, whereas sintering occurs outside of the concrete, e.g. in tunnel drainage systems. During the carbonation process, atmospheric CO_2 diffuses into the concrete pore structure, dissolves in the pore solution and subsequently reacts with the dissolved cement hydrates [50]. Portlandite dissolves and reacts with the aqueous CO_2 to form $CaCO_3$ (Eq. 1). Calcium- (aluminium)-silicate hydrate (C–(A)–S–H) carbonation involves a gradual decalcification resulting in the formation of an amorphous silica phase [51, 52]. Functioning as buffer the

amount of Ca-bearing hydrates are essential for the progression of the carbonation front.

The carbonation rate is controlled by the CO_2 concentration and the relative humidity which influences the saturation degree of the pores [53]. Therefore, the CO_2 partial pressures for accelerated test methods are higher than in nature and the relative humidity is set at an optimum ($\sim$ 55–65%). Several studies have dealt with the correlation between accelerated and natural carbonation rates of concrete [54–58] and various empirical models have been proposed. However, the applicability of these models to shotcrete has not yet been verified.

2.2.2 Chloride diffusion

Chloride diffusion in shotcrete is specially critical for seaside and undersea structures, or if shotcrete comes into contact with de-icing salts or road dust-binders (NaCl, $CaCl_2$ or $MgCl_2$) [19, 59, 60]. Cl^- diffuses inwards through the pores filled with solution, and the charge is locally balanced with the corresponding cation e.g. Na^{2+}. In the cement matrix Cl^- can be bound into hydroxyl-, carbonate-, or sulphate-AFm phases forming Cl-AFm or Friedel's salt, which acts as a chloride sink [48, 61]. The threshold of Cl^- content for Friedel's salt formation lies at a few tens of millimolar soluble chloride but depends on the precursor phase(s) [48], the hydration degree of the cement [62], the carbonation degree [63], and the cation accompanying the Cl^- [64]. Cl^- can also be sorbed to other hydrated phases like hydrotalcite and C–(A)–S–H [65, 66].

For the determination of the chloride diffusion properties of concrete natural [67] and accelerated tests [68], e.g. by means of an electrical field, are performed on solid samples. In contrast, chloride binding capacities are often determined on powdered samples [69, 70].

2.3 Clinker reduced shotcrete: influence of SCMs

Similarly to concrete, current developments in shotcrete technology include the use of SCMs to lower the clinker content in the cementitious binder [71, 72]. In addition to environmental considerations, SCMs can help to increase the durability of concrete/shotcrete exposed to certain aggressive environments [24, 27]. Pozzolanic SCMs (metakaolin, fly ash, silica fume)

react with portlandite, thereby increasing the C–(A)–S–H content in the matrix and producing lower pH pore solutions compared to pure OPC mixes [71]. Latent hydraulic SCMs, like ground granulated blast furnace slag (GGBFS), react with water to form C–(A)–S–H once they are activated by the alkaline pore solution of the concrete/shotcrete. In the case of shotcrete the use of setting accelerators may induce an earlier activation of the GGBFS [73]. Another commonly used supplementary material is powdered limestone, which forms CO_3-AFm phases, stabilises ettringite and contributes to the formation of C–(A)–S–H [9, 74–76].

Beside the possible reduction of the matrix porosity [38, 77], the presence of SCMs in shotcrete mixes is also associated with better pumpability, sprayability ('shootability') and lower rebound [27, 78]. However, the required early strength for shotcrete may be compromised if the mix is not properly optimized. Improved chloride penetration and sulphate resistance have been reported for concrete and shotcrete mixes with certain combinations of SCMs [23, 24, 27, 79]. On the other side, the substitution of clinker by SCMs could lead to lower carbonation resistance of shotcrete due to portlandite consumption and the associated reduced CO_2 buffering capacity of the cement matrix as it has been shown for concrete [80].

3 Materials and experiments

3.1 Mixtures and spraying

3.1.1 Wet-mix shotcrete

The set of analysed wet-mix shotcretes includes 12 mixtures (W1–W12) designed to fulfil different purposes, e.g. improving early strength development, packing density and durability. The samples were sprayed during two real-scale tests; W1–W8 in the first, and W9–W12 in the second series. Table 1 includes the binder composition, accelerator dosage and water to binder ratio (w/b) of the mixes. The concrete mix design, in kg/m³, can be found in Supplement Table 1. Four different cements were used: one CEM I 52.5 R, two low-C_3A cements (CEM SR0-1 and CEM SR0-2) and one CEM II/B-M (S,L,Q), according to EN197-1 [81]. Their chemical composition and physical parameters are given in

Table 2 and Supplement Table 2. The CEM II/B-M (S,L,Q) cement consists of 66% CEM I 52.5 R, 19% ground granulated blast furnace slag (GGBFS), 7% fine limestone and 8% metakaolin.

All mixtures consisted of ∼ 410 kg/m³ binder and ∼ 1800 kg/m³ aggregates (0–8 mm) (Supplement Table 1). The aggregates were in all cases dolomitic except for mix W11, where the fine size fraction (0–4 mm) consisted of silicate aggregates. An aluminium sulphate based setting accelerator and a PCE superplasticizer (0.5–1 wt% relative to binder) were used. Mix W1, with 100% cement in the binder, was taken as reference mixture for mixtures with CEM I SR0-1 cement. Mix W2, with 67% CEM I and 33% C-SCM, which is a combined product made of GGBFS, fly ash and limestone [82], was taken as the reference for the CEM I + SCM binder mixtures as it is one of the currently most used binders for shotcrete applications in Austria and recommended by the Austrian guideline for shotcrete [83]. Two of the mixes, W3 and W4, included fine limestone in order to evaluate its effect on hydration, early strength and durability. Mixes W5-W8 included limestone and further SCMs, such as GGBFS, silica fume and metakaolin, with the objective to produce particle size optimized mixes [72] and to reduce the sintering potential. W9–W11 were produced with 100% CEM II/B-M cement and differ only in the use of air entraining agent in W10, added to improve the pumpability, and in the silicate sand used for W11, to exclude a possible negative effect of carbonate sand on Ca^{2+} leaching.

For the first real-scale tests (mixes W1–W8), a CIFA Magnum MK 24 and a HSP-1 change over system by Hittmayr were used (flow rate = 20 ± 1 m³/h). At the second real-scale tests the mixtures were sprayed with a SIKA PM 500 PC spraying mobile (flow rate = 12 ± 1 m³/h; see Fig. 1). The rebound was collected and weighed after the spraying of each mix.

3.1.2 Dry-mix shotcrete

The investigated dry-mix shotcrete mixtures (D1–D10) contained either spray binder, SPB, (Table 2) or CEM I SR0-1, both with SCMs (Table 1 and Supplement Table 3). SPB is a fast setting binder based on portland-cement clinker with reduced sulfate content [83]. Mix D10 with 100% SPB was taken as the

Table 1 Wet-mix shotcrete and dry-mix shotcrete mixes: binder composition, accelerator dosage, w/b ratio and rebound; The composition of binders containing CEM II (W9-W11) is expressed as CEM I and SCMs (see Supplement Table 1 and 3 for mix-design in kg/m^3)

Mix	Cement		Mineral additions							Accelerator		w/b	Rebound
	Type	Mass (%)	GGBFS (%)	C-SCM (%)	Lime-stone p. (%)	Fine Limestone p. (%)	Silica fume (%)	Meta-kaolin (%)		Type	(wt%)[a]		(%)
Wet-mix shotcrete													
W1	CEM I SR0-1	100									8	0.48	12
W2	CEM I	67		33							8	0.45	14
W3	CEM I SR0-1	90				10					7	0.46	11
W4	CEM I	95				5					8	0.47	12
W5	CEM I	54	16		10	13	7				7	0.46	10
W6	CEM I SR0-1	60	18			15	7				11	0.45	16
W7	CEM I	54	16		10	13		7			8	0.51	11
W8	CEM I SR0-1	70	20			10					7-8[b]	0.47	n.m
W9	CEM I	66	19			7		8			7	0.50	11
W10	CEM I	66	19			7		8			7	0.49	6
W11	CEM I	66	19			7		8			7	0.49	12
W12	CEM I SR0-2	100									7	0.50	10
Dry mix shotcrete													
D1a	SPB	80	20									0.60	16
D1b	SPB	80	20									0.49	18
D2	CEMI SR0-1	90				7				p1	3	0.47	20
D3	CEMI SR0-1	90								p2	10	0.49	18
D4	CEMI SR0-1	70	15			5				p2	10	0.47	16
D5	SPB	70	20							p2	10	0.41	31
D6	SPB	70	15			5		5		p2	5	0.45	26
D7	SPB	75	15			5		5				0.50	19
D8	SPB	70	20			10						0.38	24
D9	SPB	50	30			5		5		p2	10	0.46	17
D10	SPB	100										0.50	18

[a]For wet-mix shotcrete mixtures the accelerator content was calculated relative to the binder content; for dry-mix shotcretes the used powder accelerators were counted as part of the binder

[b]Sample W8: due to technical difficulties the exact accelerator amount could not be measured

n.m not measured

reference mix for the leaching test; Mix D1b, with 80% SPB and 20% GGBFS, was taken as the reference mix for the carbonation tests. D1a consists of the same binder mixture as D1b but it was sprayed with a higher w/b, 0.60 versus 0.49. Mixtures D2, D3 and D4, made with CEM SR0-1 cement were designed to produce sulphate resistant mixes with fast setting and adequate early strength development for shotcrete applications. They were accelerated using two different types of powder accelerators: type p1 is based on ye'elemite, calcite and alunogen, type p2 consist of amorphous calcium aluminate and calcium sulphate (anhydrite). D5–D9 consisted of different combinations of spray binder and SCMs, with the aim to reduce the sintering potential of the shotcrete. All mixtures were sprayed using an Aliva 246 spraying gun, with a 3.6 l rotor (capacity of 2.5 m^3/h) and a Schuller type S-2 spraying nozzle Fig. 1. The rebound was weighed and calculated referring to the total dry-mix weight used for the spraying (Table 1).

Table 2 Mineralogical (crystalline) and chemical composition of the cements used; determined by XRD and XRF

Phases	W1-W8		W10-W11	W12	D1a, D1b, D5-D10
	CEM I	CEM I SR0-1	CEM II	CEM I SR0-2	SPB
Alite	52.2	58.2	58.0	64.8	59.1
Belite	10.8	16.9	10.7	8.1	13.8
Aluminate	11.1	2.6	9.2	0.8	11.4
Ferrite	7.1	11.9	7.5	15.2	8.2
Periclase	3.3		0.5	2.9	1.0
Anhydrite	2.2	3.9		2.0	
Bassanite	3	2	2.4	1.6	1.2
Arcanite	2.1		0.7	0.5	0.6
Calcite	4.7	3.9	7.5		0.5
Gypsum	1.5		1.7	0.7	
Portlandite	0.5	0.5			2.5
Dolomite	1.4		1.2	1.1	0.8
Quartz	0.2		0.4	0.1	
Aphthitalite		0.2			0.7
Langbeinite			0.1		
Free CaO				1.9	0.3
Oxides (wt%)					
LOI	3.4	2.8		2.0	1.8
Na_2O	0.3	0.3	0.2	0.9	0.7
MgO	4.0	1.1	3.3	3.7	2.0
Al_2O_3	5.4	3.1	9.7	3.4	6.1
SiO_2	19.1	21.4	25.5	19.5	20.6
P_2O_5	0.1	0.1	0.2		0.3
SO_3	3.1	2.4	3.5	3.3	1.2
K_2O	0.9	0.4	0.5	0.7	0.7
CaO	60.8	63.7	54.0	61.0	63.4
TiO_2	0.2	0.2	0.5	0.2	0.3
MnO	< 0.1		0.3	0.1	0.1
Fe_2O_3	2.7	4.5	2.1	5.3	2.8

wet-mix spraying   dry-mix spraying   sample preperation

Fig. 1 Impressions of the sample production: from the spraying process (wet and dry) to the aftertreatment and drill core extraction

3.2 Durability tests

The following durability parameters were determined: (1) sintering potential, (2) natural (sheltered) and accelerated carbonation rate, (3) Cl^- diffusion coefficient (Table 3). Additionally, Cl^- diffusion profiles and distribution as well as the Cl^- binding capacity were analysed for selected mixtures. All correlation statistics were computed with Origin Pro 2019 (9.6.0.172). For each correlation, the determination coefficient (R^2) as well as the degree of freedom (df) are listed and the 95% confidence interval is plotted.

3.2.1 Sample preparation

The shotcrete mixtures were sprayed into panels (see Fig. 1) from which drill cores (100 mm Ø) were taken after 24 h and stored underwater (T = 20 °C). Only the cores for the SP test were cured in boxes with RH > 95% and T = 20 °C. Right before the start of the experiments (leaching, carbonation & chloride diffusion tests), smaller cores, with a diameter of 50 or 70 mm, were drilled out from the inner part of the 100 mm specimens. Additionally, 15 mm were removed from the upper and lower end of the cylinders. For the chloride diffusion mappings, prisms ($\sim 50 \times 50 \times 70$ mm) were cut out of the 100 mm drill cores. For the chloride binding capacity tests and for the additional analytical tests, a ~ 30 mm slice was cut from a 50 mm drill core, subsequently dried in vacuum and crushed to < 125 μm in a vibration disk mill.

3.2.2 Sintering potential (SP)

The leaching and sintering potential of the shotcrete mixes was determined by means of the 'sintering potential' (SP) test, described in the guideline "sintering potential determination" [84]. As recommended, the test was started when the samples were 56 days old. Each drill core (Ø = 50 mm; l = 100 mm; n = 2–3) was immersed in a 2.5 l test box filled with demineralized water, keeping a water:solid ratio of 4:1. The test was divided into three cycles with the duration of 24 h for the first, 48 h for the second and 120 h for the third cycle. The leachate was decanted after each cycle and after the first two, the water was renewed in the boxes. The decanted leachate pH-value and electrical conductivity were measured using a Multi 3420 WTW pH meter. For the determination of the Ca^{2+} in the leachates the solutions were acidulated (pH = 3–4) with a concentrated hydrochloride acid to dissolve potentially precipitated carbonates and ensure that the total leached Ca^{2+}-concentration was measured. The Ca^{2+} leached from the wet-mix shotcrete was measured by means of ICP-OES (PerkinElmer Optima 8300) and for the dry-mix shotcrete titration (calconcarboxylic acid indicator, 0.05 mol EDTA) was used. Selected dry-mix samples were measured by both methods for further validation, obtaining a maximum deviation in the Ca^{2+} value of 3 mg/l. The Ca^{2+} values obtained from the three cycles were summed up and then expressed as kg calcium per ton of shotcrete. The SP value was determined from the average of 2–3 drill cores.

3.2.3 Carbonation

Drill cores (Ø = 50 and 70 mm; l ≥ 130 mm) for natural and accelerated carbonation were taken after 65 days of curing and subsequently stored in a climate chamber (20 °C; 65% RH) for 7 days to adjust the sample moisture content to the conditions in the CO_2 chamber. The diameter was increased to 70 mm after the first real-scale test to ensure that the carbonation depth would never be higher than the radius.

The accelerated carbonation test was performed according to ONR CEN/TS 12390–12 [85] and the fib Model Code for Service Life Design [86]. After preconditioning, the cores were placed for 140 days in an automatic accelerated carbonation chamber with a CO_2 concentration of 2 volume%, RH of 65% and temperature of 20 °C. The lack of carbonation before the start (0d) was confirmed on selected samples. Carbonation depths were measured after 28, 70 and 140 d. 30–40 mm long disks were split perpendicularly to the cylinder axis, which is equal to the spraying direction, obtaining two freshly split surfaces of 50–70 mm diameter. Specimens from mixes W9–W12 and D1a–D9 were also split parallel to the spraying direction (Fig. 2a) to analyse possible effects related to spraying layers. A $\sim$ 1wt.% phenolphthalein-ethanol solution was sprayed on the fresh surface. The visual transition shown by phenolphthalein from colourless to fuchsia in the pH-area of 8.2–10 [52], was used to determine the depth of the carbonation front. After 60 ± 15 min, around eight

Table 3 List of executed durability tests and additional parameters measured

Mixture	Sintering potential n	Acc. carbonation n	Nat. carbonation n	Cl⁻ diffusion profiles n	Cl⁻ diffusion mapping n	Cl⁻ binding n	Porosity n	Portlandite n
W1	3	2	n.m	2	n.m	4	2	1
W2	3	2	n.m	2	n.m	4	2	1
W3	3	2	n.m	2	1	4	3	1
W4	3	2	n.m	2	1	4	3	1
W5	3	2	n.m	2	n.m	4	2	1
W6	3	2	n.m	2	n.m	4	2	1
W7	3	2	n.m	2	n.m	4	3	1
W8	3	2	n.m	2	n.m	4	2	1
W9	2	3	n.m	2	1	n.m	1	1
W10	2	3	3	n.m	n.m	n.m	1	1
W11	2	3	3	n.m	n.m	n.m	1	1
W12	2	3	3	n.m	n.m	n.m	1	1
D1a	2	3	3	n.m	n.m	n.m	1	1
D1b	2	3	3	n.m	n.m	n.m	1	1
D2	2	3	3	n.m	n.m	n.m	1	1
D3	2	3	3	n.m	n.m	n.m	1	1
D4	2	3	3	n.m	n.m	n.m	1	1
D5	2	3	3	n.m	n.m	n.m	1	1
D6	2	3	3	n.m	n.m	n.m	1	1
D7	2	3	3	n.m	n.m	n.m	1	1
D8	2	3	3	n.m	n.m	n.m	1	1
D9	2	3	3	n.m	n.m	n.m	1	1
D10	3	n.m	n.m	n.m	n.m	n.m	n.m	n.m

n number of samples; *n.m* not measured

carbonation depth measurements were taken for each core by means of a caliper (Fig. 2b). For samples with visual observed outliers (see chapter visual observation in results) more measurements (up to 16) were conducted. Outliers were not considered for the calculation of the average values of each drill core for the determination of the carbonation rate.

For the natural carbonation test, the dry-mix shotcrete samples were stored outside in Graz (Austria), sheltered from the rain, from May 2018 until July 2019 and the wet-mix shotcretes from July 2018 until August 2019. During this time, the average temperature was around 12 °C and the relative humidity ∼ 69% (see Supplement Fig. 1). After 395 and 413 days the carbonation depth of samples W9–W12 and D1a–D9, respectively, was measured as described above. The 'carbonation rate', K, was obtained from

the slope of the linear regression of the carbonation depth versus the root of time (Eq. 2; Fig. 2c).

$$K = \frac{\Delta carbonation\,depth\,[\text{mm}]}{\Delta\sqrt{time}\,[\text{d}]} \qquad (2)$$

3.2.4 Chloride diffusion coefficient

The chloride diffusion coefficients were determined for mixtures W1–W8 according to EN 12390–11 [67]. For each mixture one drill core (50 mm Ø) was retrieved after 75 days of underwater storage. After storing the samples for 16 h in a $Ca(OH)_2$ solution the specimens became water saturated under vacuum. Subsequently, the specimens were coated with a Cl⁻ free epoxy resin (Epoxy 2000 from Cloeren Technology), dried and cut crosswise in half. Thereafter the

Table 4 Summary of results obtained from additional tests: portlandite content, critical pore size and pore volume and the durability tests: SP sintering potential; K_{acc} accelerated carbonation rate; K_{nac} natural carbonation rate; D_{nss} Chloride diffusion coefficient. The standard error or standard deviation was determined if the sample number was ≥ 3

Mixtures	Portlandite		Critical pore Ø	Pore volume	SP	K_{acc}	K_{nac}	D_{nss}
	(%/g concr.)	(%/g cement)	(nm)	(%)	(kg/t)	(mm/$\sqrt{d}$)	(mm/$\sqrt{a}$)	$*10^{-12}$ (m^2/s)
Wet – mix shotcrete								
W1	1.8	10.3	18.9	8.4	0.66	0.6 ± 0.0	n.m	5.3
W2	0.9	7.4	18.5	8.5	0.41	1.1 ± 0.0	n.m	3.0
W3	1.3	8.5	27.8 ± 1.6	7.8 ± 1.4	0.70	0.6 ± 0.0	n.m	9.1
W4	1.9	11.7	26.3 ± 4.1	6.8 ± 1.0	0.63	1.0 ± 0.1	n.m	6.6
W5	0.4	4.6	21.9	7.7	0.31	1.3 ± 0.0	n.m	1.4
W6	0.2	1.9	21.5	8.0	0.34	1.1 ± 0.2	n.m	2.0
W7	0.6	6.3	27.2 ± 1.5	7.7 ± 1.9	0.31	1.3 ± 0.1	n.m	3.4
W8	1.1	9.3	24.5	6.6	0.43	1.1 ± 0.1	n.m	2.4
W9	0.8	6.8	25.1	6.8	0.30	0.8 ± 0.0	n.m	1.4
W10	0.4	3.2	26.9	8.0	0.30	0.9 ± 0.1	4.2 ± 0.2	n.m
W11	0.9	6.8	23.6	9.0	0.34	0.9 ± 0.1	3.9 ± 0.2	n.m
W12	1.8	10.0	41.5	8.8	0.79	0.7 ± 0.1	3.0 ± 0.3	n.m
Dry – mix shotcrete								
D1a	2.1	17.2	56.5	9.7	0.65	0.9 ± 0.1	3.1 ± 0.4	n.m
D1b	2.5	20.3	65.4	8.2	0.55	0.6 ± 0.0	2.7 ± 0.2	n.m
D2	2.8	20.3	38.0	8.6	0.87	0.4 ± 0.0	1.8 ± 0.2	n.m
D3	2.5	16.3	44.9	8.5	0.80	0.6 ± 0.1	2.8 ± 0.1	n.m
D4	2.0	16.6	37.8	7.0	0.57	0.6 ± 0.1	2.4 ± 0.3	n.m
D5	1.3	10.5	53.1	7.7	0.52	0.5 ± 0.1	2.3 ± 0.0	n.m
D6	0.6	5.0	39.0	9.6	0.32	1.4 ± 0.1	5.2 ± 0.3	n.m
D7	1.4	12.5	55.6	8.2	0.44	0.6 ± 0.0	2.6 ± 0.1	n.m
D8	1.9	17.6	45.8	8.6	0.50	0.4 ± 0.0	1.6 ± 0.2	n.m
D9	0.8	9.1	48.7	8.4	0.33	0.8 ± 0.1	3.6 ± 0.2	n.m
D10	2.1	13.4	n.m	n.m	0.69	n.m	n.m	n.m

n.m. not measured

Fig. 2 **a** Double splitting of carbonation samples; **b** phenolphthalein spraying and carbonation depth measurement; **c** determination of carbonation rate K = slope of linear regression
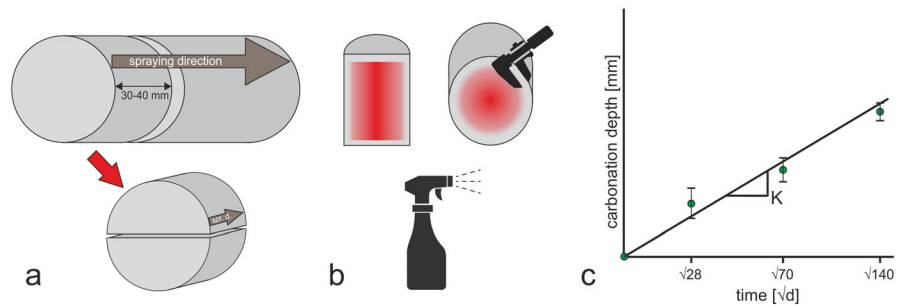
samples were stored in boxes filled with a 3% NaCl solution for 90 days. After the exposure, 7 cross-sections with an average thickness of 3 mm were cut from the sample. The slices were dried at 40 °C and then powdered using a vibration disc mill (< 125 μm). The acid soluble Cl^--content was determined by placing 0.5 g of shotcrete powder in 2 g of 2% HNO_3 solution for 5 min and subsequent filtering using 0.45 μm cellulose acetate filters. The obtained liquid sample was diluted 1:200 with MilliQ water (omega = 18.2) and the Cl^- content was subsequently measured by ion chromatography (Dionex ICS 3000; analytical error < 3%). The initial Cl^- content of the concrete mixture (C_i) was measured in the same way. The obtained Cl^- concentration values for the various depths were used to calculate the diffusion coefficient (D_{nss}) and the Cl^- surface concentration (C_S) using a least-squares fitting method (Eq. 3).

$$C_X = C_i + (C_s - C_i) \cdot \left(1 - erf\left(\frac{x}{2 \cdot \sqrt{D_{nss} \cdot t}} \right) \right)$$
(3)

C_X measured chloride concentration at depth x [wt%]. C_i initial chloride concentration of concrete [wt%]. C_S chloride surface concentration [wt%]. x distance from the sample surface to the middle of the layer [m]. D_{nss} non steady state diffusion coefficient [m^2/s]. t time [s]

3.2.5 Chloride diffusion profiles and distribution

The spatial distribution of chloride was mapped in mixes W3, W4 and W9 by means of electron microprobe analysis. After 75 days of water storage, prisms were placed in a 3% NaCl solution for 90 days. Thereafter, a cross-section was cut out of each prism, embedded in Cl^- free resin (Epoxy 2000 from Cloeren Technology) and subsequently polished on diamond grinding disks with ethanol as coolant. The chloride concentration and diffusion depths were analysed using a JEOL JXA8530F Plus Hyper Probe electron microprobe, equipped with a field emission gun. Elemental mappings of Cl^- were recorded at 15 kV and 50 nA, a dwell time of 15 ms and a step size of 10 μm. Quantification was performed against a tugtupite mineral standard. From the mappings, elemental

Cl^- profiles were calculated exclusively for the cement matrix by not considering the aggregate grains in the calculation. Thereto, elemental cut-off concentrations were determined to ensure the exclusion of the pixels corresponding to aggregates.

3.2.6 Chloride binding

The Cl^- binding capacity of the shotcrete was analysed by immersing powdered samples (< 125 μm) of mixes W1-W8 in chloride solutions. Four sodium-chloride solutions with different concentrations were used: L1 = 35 mg/l, L2 = 350 mg/l, L3 = 3.5 g/l, L4 = 35 g/l. The L1 Cl^- concentration is similar to that found in drinking water; the L4 Cl^- concentration reflects the average value for ocean water. 10 g powder of each concrete mixture were put into each of the four solutions, which means in total 32 tests were performed. After one month, the tests were ended, and the solid samples were analysed by XRD (PANalytical X'Pert PRO). For the quantification of the AFm phases and Friedel's salt, Rietveld analysis was conducted for selected samples, and the peak areas were determined.

3.3 Additional analysis methods

The chemical composition of the shotcrete mixes, after 56 days of underwater curing, and the used raw materials were analysed quantitatively by X-ray fluorescence (XRF; PW 2404) using borate glass pellets. The mineralogical compositions of the samples were determined by means of X-ray diffraction (XRD; PANalytical X'Pert PRO; Co X-ray tube; 40 kV; 40 mA) and Rietveld analysis. Additionally, thermogravimetry analyses (TG; Perkin Elmer STA 8000; 10 °C min^{-1}) were carried out to determine the portlandite formed during hydration and bound water content in 0.08 g powdered concrete samples after 56 days of underwater curing. The portlandite content per gram cement was also calculated by considering the determined water content and the ratio between aggregates plus SCMs to cement content in the concrete mixture. The overall porosity (e.g. pore volume and critical pore radius) was determined by

mercury intrusion porosimetry (Thermo Scientific Pascal 140 and Pascal 240 series porosimeters, see also Steindl et al. 2020 [24] and Supplement Fig. 2).

4 Results

A summary of the results obtained is presented in Table 4. The results include those from the durability tests (sintering potential, carbonation rates and chloride diffusion coefficient) as well as those from the additional tests (portlandite content, critical pore diameter and pore volume).

4.1 Ca^{2+} leaching

According to the SP values, the dry-mix shotcretes showed higher leaching potential compared to the wet-mix shotcretes. In addition, mixtures with higher cement content showed higher leaching values. This can be clearly seen in W1, W3, W4 and W12 wet-mix shotcretes, exhibiting SP values between 0.63 and 0.79 kg/t, and in D10, D2 and D3 dry-mix shotcretes, with SP values ranging from 0.69 to 0.87 kg/t. Fine limestone powder substituted for cement, like in W3 led to higher Ca^{2+} leaching rates compared to W1. However, dry- and wet-mix shotcrete mixtures containing pozzolanic and latent hydraulic SCMs featured reduced SP values, even in the presence of limestone. The fine carbonate aggregates (0–4 mm) did not negatively influence the SP values: mix W9, with dolomite sand, and W11, with quartz sand showed both a very low Ca^{2+} leaching. Higher w/b ratios in dry-mix shotcrete led to higher SP value, as shown by mixes D1a, with w/b = 0.60 and SP 0.65 kg/t, and D1b, with w/b 0.49 and SP 0.55 kg/t.

4.2 Carbonation

4.2.1 Visual observations

The phenolphthalein test revealed some inconsistencies in the carbonation depth results of samples W1–W12, evidenced for example in the case of sample W1, where the depth after 28 d was higher than after 70 d. This lack of consistency was found in samples where the carbonation depth was not similar all around the surface (examples in Fig. 3). For the phenolphthalein test, W1–W8 cores were split perpendicular to the spraying direction; to complement the measurement and detect possible inhomogeneities due to the spraying process, drill cores of W9–W12 and D1a–D9 were additionally split parallel to the spraying direction, allowing for the observation of different spraying layers. The term layer in the following sections always refers to areas with weaker properties (mechanical or in terms of durability). In the four wet-mix shotcretes W9–W12, layers with higher carbonation depth, up to four times, could be observed (see Fig. 3). Due to that, obvious outliers in the carbonation depth data set of W1–W8 were excluded from the calculations. No layering was witnessed in any of the dry-mix shotcrete cores.

4.2.2 Accelerated carbonation rates

Differences were observed in the accelerated carbonation rates of dry- and wet-mix shotcretes: dry-mix shotcrete carbonation rates were between 0.4 and 0.9 mm/$\sqrt{}$d (except D6 with 1.4 mm/$\sqrt{}$d), which is lower than the wet-mix shotcrete results (between 0.6 and 1.3 mm/$\sqrt{}$d). Wet-mix shotcretes made with CEM I (W2, W4, W5, W7) showed higher carbonation depths compared to those made with CEM I SR0-1 and 2 (W1, W3, W6, W8, W12; Supplement Fig. 3). In both, dry- and wet-mix shotcretes, mixtures with higher cement content (W1, W12, W4, W3, D2) showed lower carbonation rates. D8, produced with SPB, GGBFS and limestone, showed one of the lowest carbonation rates, 0.4 mm/$\sqrt{}$d, despite the lower cement content in the binder. The highest carbonation rates were observed in wet-mix shotcrete mixtures made with CEM I, low cement content and pozzolanic SCMs (W5 and W7), with 54% cement in the binder and rates of 1.3 mm/$\sqrt{}$d. Similarly to the SP-value, higher w/b values ($\Delta = 0.11$) in dry-mix shotcrete led to an increase of the carbonation rate ($\Delta = 0.3$ mm/$\sqrt{}$d).

4.2.3 Natural carbonation rates

Wet-mix shotcrete drill cores from the second real-scale test (W9–W12) and the dry-mix shotcretes (D1a–D9) were stored outside sheltered from the rain for more than one year. Similar trends as in the accelerated carbonation were observed: dry-mix shotcretes showed lower carbonation rates than wet-mix shotcretes, with the exception of D6, exhibiting
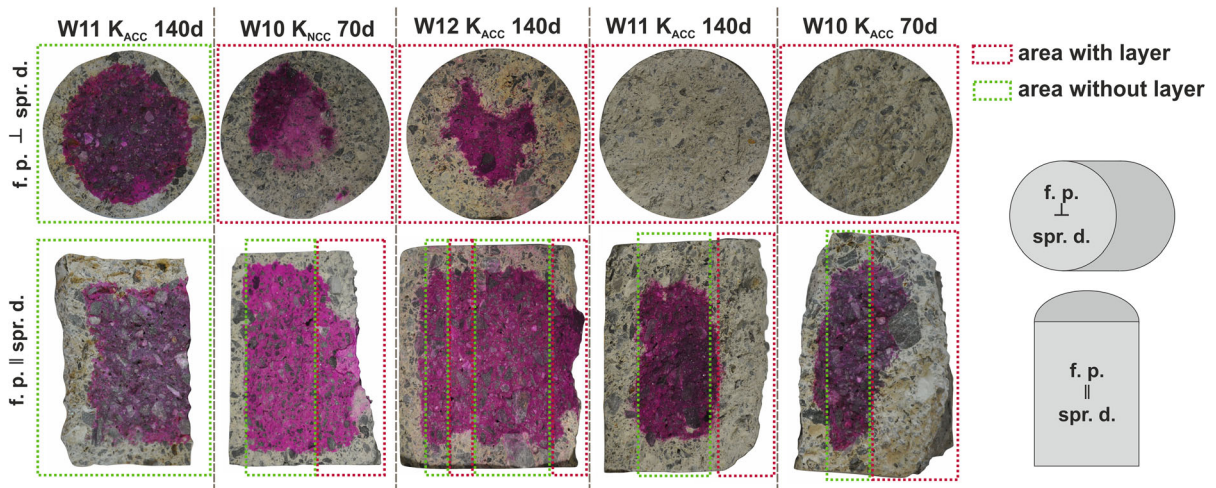
Fig. 3 Carbonation tests showing the presence and absence of layers. Cores broken perpendicular to the spraying direction (spr. d.) often break at layers and therefore exhibit higher carbonation depths. In the fracture planes (f. p.) parallel to the spraying direction both non-layered and layered areas are visible

the highest carbonation rate of 5.2 mm/$\sqrt{a}$ (Table 4). Mixtures with higher cement contents, W12, D2, and D3, showed lower carbonation rates and again, D8, despite having only 70% cement in the binder, showed the lowest rate, 1.6 mm/$\sqrt{a}$.

4.3 Chloride diffusion and binding

4.3.1 Diffusion coefficient

Diffusion coefficients were determined for 9 of the wet-mix shotcretes and ranged from 1.4×10^{-12} m^2/s to 9.1×10^{-12} m^2/s (Table 4). Mixtures containing CEM I did not show lower chloride diffusion than mixtures with CEM I SR0-1 even though the Al$_2$O$_3$ content of CEM I is higher ($\Delta = 2.3$ wt%). The two mixtures with only limestone substitution, W3 and W4, showed the highest D_{nss} values: 6.6×10^{-12} m^2/s for W4 and 9.1×10^{-12} m^2/s for W3 (Fig. 4; Supplement Fig. 4). In general, samples with higher cement contents (W1, W3, W4) exhibited higher D_{nss} values and mixtures with higher cement substitution (W5, W6, W8 & W9) featured the lowest diffusion depths. Mix W7 with low cement content showed very different values in the two cores analysed: in the first core D_{nss} was 1.9×10^{-12} m^2/s, whereas in the second one it increased to 6.8×10^{-12} m^2/s.

4.3.2 Chloride distribution

Chloride distribution mappings and the mean concentration profiles for mixtures W3 (90% CEM SR0 and 10% fine limestone fL), W4 (95% CEM I and 5% fL) and W9 (100% CEM II) are shown in Fig. 4, together with the mean chloride concentration profiles resulting from the test according to EN 12390–11. In the prism of W3 and W4 ($\sim 50 \times 50 \times 70$ mm) the chloride has penetrated all through the samples with a gradual decrease. The profile of W9 shows a high chloride concentration between a depth of 1.2 and 3.7 mm followed by a steep decrease up to the initial concentration at a depth of 10 mm. The distribution mappings also show the leaching zone, which is depleted in chloride ions (Fig. 4). The leaching is apparent in all three samples, but the zone is relatively small in W4 compared to W3 and W9. When comparing the profiles from the mappings with the profiles from the chloride diffusion coefficient determination, the trends are similar but due to the unidirectional diffusion the chloride concentration decreases to a lower content in the drill cores. In W3 the fluctuation of the mean values indicates locally higher differences in the chloride concentrations which is also visible in the mapping. W4 and W9 on the other side exhibit a smoother distribution.
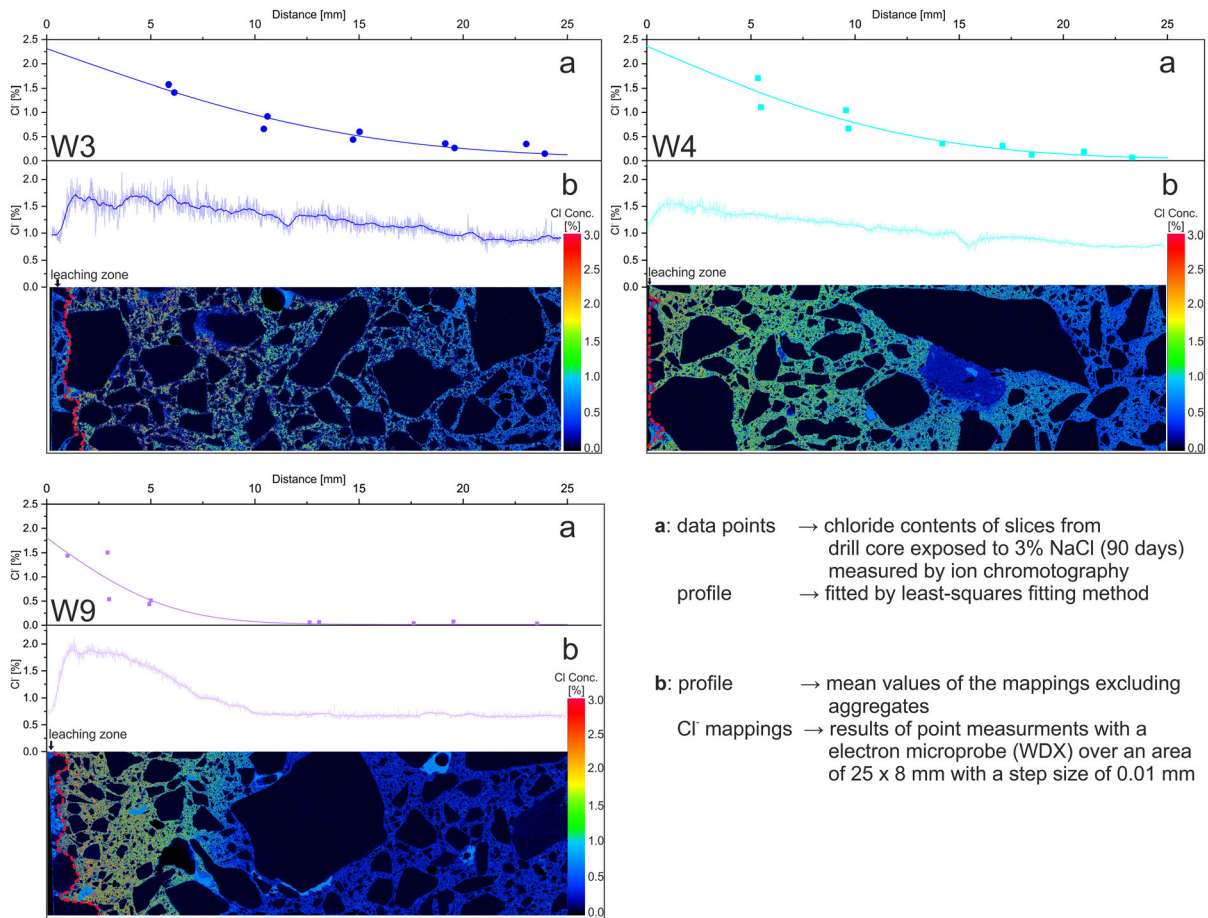
Fig. 4 **a** Cl$^-$ diffusion curves from standard test EN 12390–11; **b** mappings of the microprobe and the determined mean profiles. The end of the leaching zone is marked with a red dashed line

4.3.3 Chloride binding

The analyses of the altered solid samples show that Friedel's salt formed in all 8 shotcrete powders stored in solution L4 (35 g/l NaCl, 0.6 M Cl$^-$) and in most cases in solution L3 (3.5 g/l NaCl, 60 mM Cl$^-$) (Fig. 5 and Supplement Fig. 5). In solution L2 (350 mg/l NaCl, 6 mM Cl$^-$) a peak shift from CO$_3$ - AFm into the direction of Friedel's salt is visible in some of the powdered shotcrete mixtures. In solution L1 (35 mg/l NaCl, 0.6 mM Cl$^-$) no peak shift but an increase in crystalline AFm was observed in all samples (Fig. 5). This result fits with findings from Birnin-Yauri and Glasser [87], who stated that a chloride concentration of ~ 14 mM is needed to form pure Friedel's salt and more than ~ 2 mM of Cl$^-$ is needed to incorporate significant amounts of Cl$^-$ in hydroxyl AFm. In all four solutions, portlandite

disappeared in most mixtures and the dolomite content decreased.

Mixtures with lower initial AFm content (Supplement Table 4) formed less Friedel's salt, with the exception of W3 which formed more Friedel's salt than expected from the initial crystalline AFm content (see Fig. 6a). W3 was the sample where the crystallization of AFm after immersion in L1 was more evident (Fig. 5). The amount of AFm in the samples immersed in L1, calculated as the area of the AFm main peak (between 12 and 14°), correlates well with the amount of Friedel's salt formed in samples immersed in L4 (see Fig. 6b), including the sample W3.

4.4 Portlandite content and porosity

The total portlandite contents of the shotcrete samples—measured by thermogravimetric analyses—were in a range between 0.4 and 2.8 wt% per gram concrete and between 1.9 and 20.3 wt% per gram cement (Table 4). Dry-mix shotcretes contained higher amounts of portlandite in the matrix compared to wet-mix shotcrete mixtures, 5–20% versus 2–12% per g cement. In the two groups, higher cement contents (W1, W4, W12, D2) led to higher portlandite contents in the binder. Mixes containing pozzolanic SCMs exhibited very low portlandite concentrations within the two groups (W5–W7, W9–W11, D6, D7 and D9). Reducing the w/b ratio led to an increase in the portlandite content (see mixes D1a and D1b in Table 4), whereas the addition of an amorphous calcium aluminate (+ calcium sulphate) powder accelerator (D3, D4, D5, D6 and D9) resulted in lower portlandite contents. It is worth noting that, due to the rebound and the changes it caused on the aggregate/paste ratio in the shotcrete matrix, the portlandite values per gram cement may be overestimated.

The measured pore volumes of the shotcrete samples ranged from 6.6 to 9.7 vol%. Dry-mix

Fig. 5 XRD analyses of W1 and W3 powders before (initial) and after storage in the four solutions L1, L2, L3 and L4; the transformation from monocarboaluminate AFm (m AFm) and hemicarboaluminate AFm (h AFm) with increasing Cl⁻ concentrations into Friedel's salt (fs) can be observed by a peak shift. *ett* ettringite, *p* portlandite, *dol* dolomite;
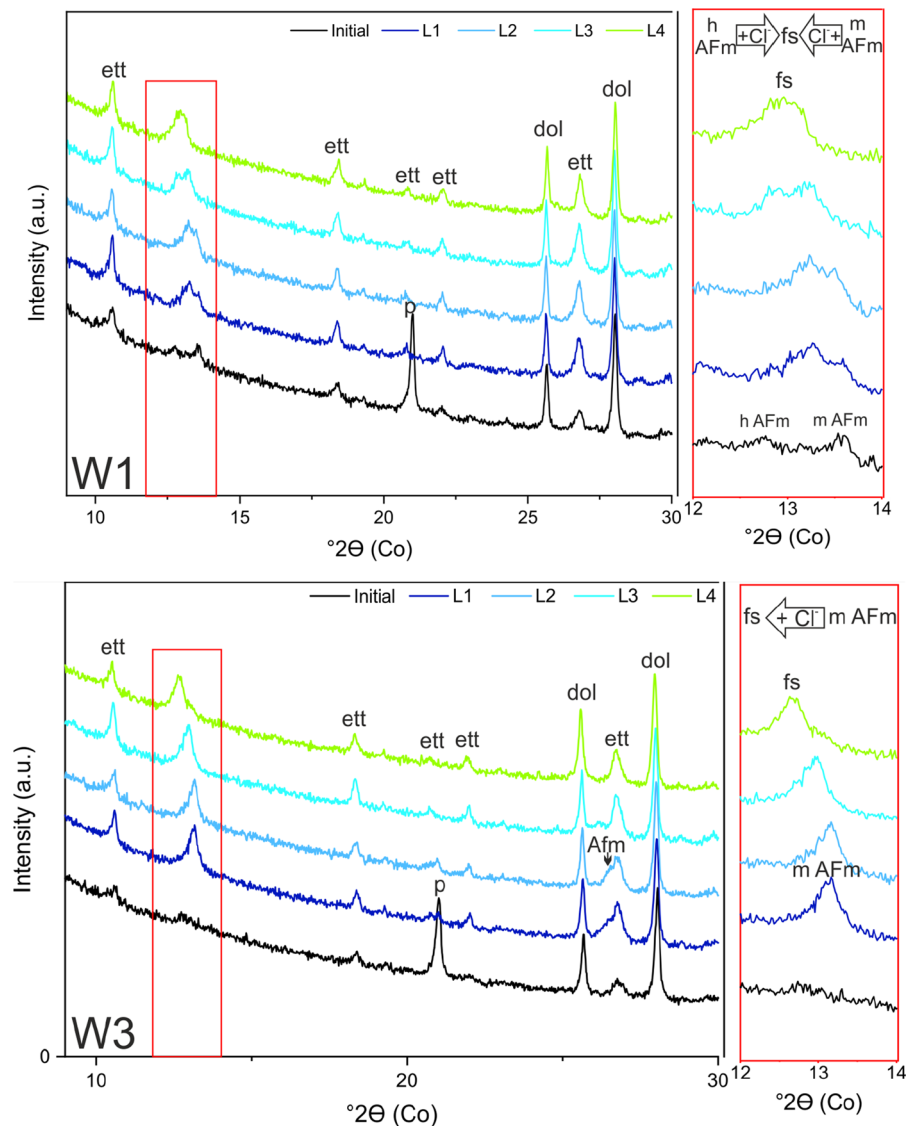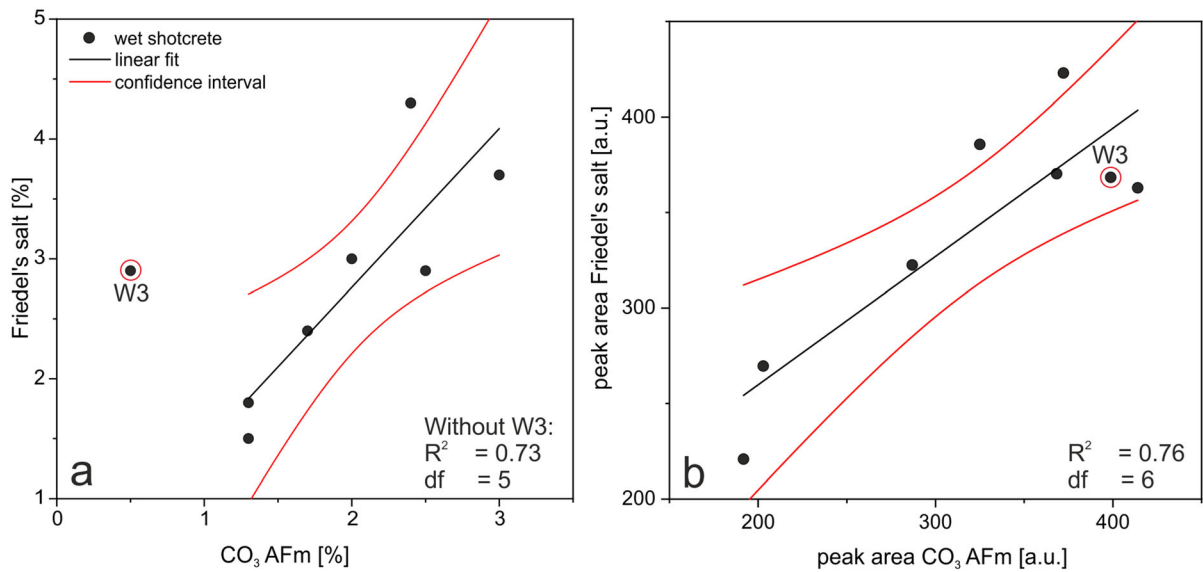
Fig. 6 **a** Initial mono and hemicarbonate AFm content versus newly formed Friedel's salt in L4 (Rietveld analyses); **b** peak area of AFm phases in L1 versus peak area of Friedel's salt in L4

shotcrete mixtures exhibited larger critical pore diameters and broader pore size distributions compared to the wet-mix shotcretes, especially in the case of D1b, D7, D8 and D9. Further results related to the porosity of the samples can be found in Steindl et al. 2020 [24].

5 Discussion

Shotcrete durability is influenced by chemical and physical factors. The high number of mixtures analysed, in total 23, enables correlations between the chemical properties and the durability performance of shotcrete, in particular the leaching, sintering, carbonation and chloride penetration resistance.

5.1 Influence of binder composition and resulting phase assemblage

5.1.1 Influence of portlandite content and reactive CaO

The results from this study clearly indicate that the portlandite content in shotcrete influenced leaching, sintering and carbonation processes. Furthermore, the portlandite content correlates linearly with the SP-value ($R^2 = 0.76$) and the accelerated carbonation rate

($R^2 = 0.51$) (Fig. 7). The good correlation for SP suggests that within the test duration of 8 days, mainly portlandite dissolution contributed to the leached Ca^{2+}. Thus, lower portlandite contents resulted in lower SP-values. Contribution of C–(A)–S–H decalcification is regarded as very minor due to the limited test duration. This is in agreement with the literature for conventional concrete: with decreasing Ca^{2+} concentration in the pore solution (1) first portlandite dissolves, (2) then ettringite, AFm and hydrogarnet decalcify, and (3) C-(A)-S–H incongruently dissolves [19, 36–39]. The observed lower linear correlation for accelerated carbonation rates—increasing K_{ACC} with decreasing portlandite content—indicates that other factors like porosity and its change during carbonation, as well as other phases (C–(A)–S–H; ettringite) have played a more important role in the carbonation process [88].

The ratio of water to reactive CaO, w/CaO$_{reactive}$, was calculated (Supplement Table 5) according to Leemann et al. 2015 [89] in order to analyse the influence of all Ca-bearing hydrates on the leaching and carbonation behaviour. The CaO$_{reactive}$ represents the amount of CaO in the binder only neglecting CaO from limestone additions. The CaO$_{reactive}$ value was calculated by summing up the CaO contents—respectively to the binder—of the used CEM I/SPB and the slag. The water to CaO$_{reactive}$ ratio considers the water
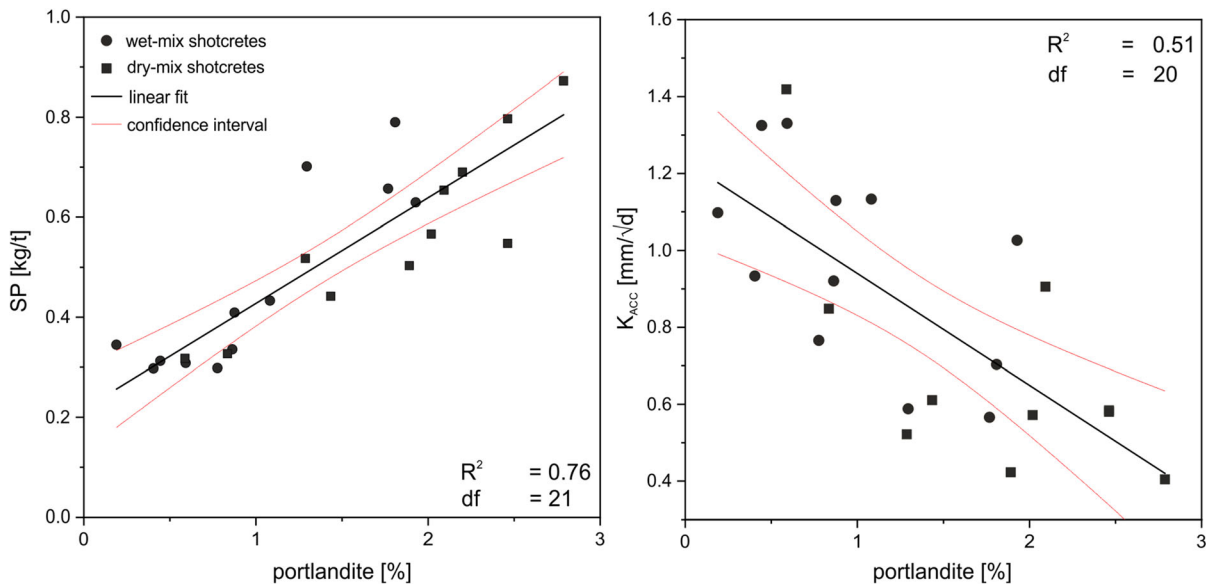
Fig. 7 Correlation of portlandite contents of shotcretes with the SP-values and the accelerated carbonation rates

available for hydration and it is therefore an indicator for the potential amount of Ca- bearing hydration phases that can be formed. The accelerated carbonation rate of the shotcretes correlates linearly with the $w/CaO_{reactive}$, with only one outlier (D6) (Fig. 8). The disagreement between $CaO_{reactive}$ and accelerated carbonation rate in sample D6 may be related to the high rebound measured for this sample (Table 1), which may have led to a significant error in the calculation of the $w/CaO_{reactive}$ value. In the future, more mixtures with $w/CaO_{reactive}$ ratios between 1.05 and 1.2 may be included to increase the reliability of the correlation. The weaker correlation obtained, compared to the one reported by Leemann et al. [53, 89] for conventional OPC-based concrete may be due to the fact that the error for the determination of $w/CaO_{reactive}$ is higher for shotcrete—due to the rebound—than for conventional concrete. The correlation was only conducted for the accelerated and not the natural carbonation rates because of the higher number of mixtures tested. The SP values do not correlate linearly with the $w/CaO_{reactive}$ values ($R^2 = 0.39$) but a trend of decreasing SP values with increasing $w/CaO_{reactive}$ was observed (Supplement Fig. 6).
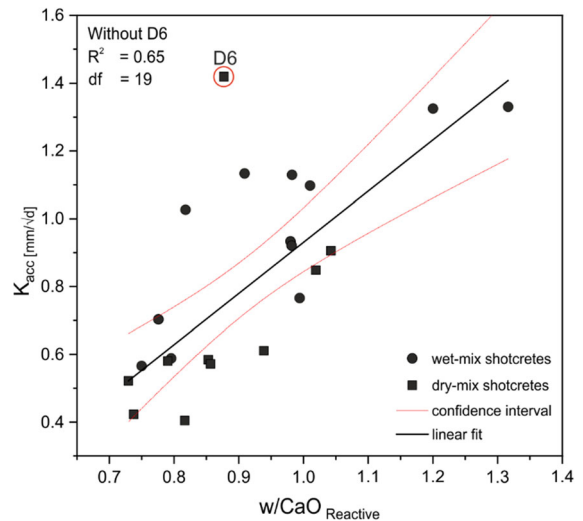
Fig. 8 Correlation between accelerated carbonation rate and $w/CaO_{reactive}$

5.1.2 Influence of binder composition

Wet-mix shotcrete results show that the presence of both silica fume and metakaolin led to a reduction of the sintering potential. In contrast, the addition of fine limestone, in the absence of other SCMs, produced mixes with higher SP (W3 and W4). When limestone was mixed with GGBFS, and in some cases also with metakaolin or silica fume, no negative effect was

observed in terms of leaching and sintering. For example, W5–W6 and W9–W11, containing all GGBFS, metakaolin or silica fume and limestone, showed the lowest SP values, 0.30–0.34 kg/t.

To better evaluate the effect of SCMs on the sintering potential, a "cement SP" value was calculated based on the cement content in the binder excluding SCMs. This value is obtained as shown in Eq. 4 where $SP_{100\%cem}$ is the value measured in samples with 100% cement and no SCMs in the binder (W1 and D10). These $SP_{100\% \, cem}$ values were used to calculate the "cement SP" of W3, W6, W8 and D1a, D1b, D7, D8 (Table 5). The "cement SP" corresponds to the SP value assuming inert SCMs not affecting the Ca^{2+} leaching behaviour. Even though the approach neglects the changes due to the different w/b ratios (ranging from 0.4 to 0.5), it provides an idea of the role played by the various SCMs.

$$cement \, SP \left[\frac{kg}{t}\right] = cement \, in \, binder \, [\%]$$
$$\cdot \, SP_{100\% \, cem}\left[\frac{kg}{t}\right] \qquad (4)$$

In the sample containing limestone powder, W3, the measured value is much higher than the calculated cement SP value, which could be related to partial dissolution of the fine limestone powder during the test or to the resulting pore size distribution. Similarly, the latter could also explain the higher Cl^- diffusion rate of this mixture. Mix W8, with 70% CEM I, 20% GGBFS and 10% fine limestone powder in the binder, shows a lower SP than expected. Despite the negative effect of limestone, the presence of GGBFS contributes to reduce the SP value in the wet-mix shotcrete mixture more than only due to dilution effects. In dry-mix shotcrete mixes (D1b, D8), however, GGBFS seems to just have a dilution effect for the SP at the

time of testing (56 days of curing). This could be related to the fact that in wet-mix shotcrete GGBFS reacts faster than in this type of dry-mix shotcrete, where no accelerator was used [73]. In mixtures W6 and D7, which contained pozzolanic and latent hydraulic SCMs, the measured SP values are lower than expected, presumably due to the consumption of portlandite, changes in the pore structure and the dilution effect. The pozzolanic reaction of silica fume does not just trigger C-(A)-S–H formation, it also modifies its internal structure, thereby increasing the average silicate chain length and stabilising Ca^{2+} [77].

Opposite trends, compared to the Ca^{2+} leaching ones, are observed for the carbonation resistance of shotcrete. The substitution of clinker by SCMs had a negative effect on the carbonation resistance due to reduction of the $CaO_{reactive}$ content. The modification of the microstructure due to SCMs substitution, including porosity reduction, does not seem to compensate for the resulting lower buffering capacity of portlandite and C–(A)–S–H, which slows down the penetration of the carbonation front.

Regarding the chloride penetration resistance, the presence of SCMs had a positive effect: samples with high clinker content exhibited the highest diffusion coefficients, as illustrated in the Cl^- mapping from Fig. 4, where mixture W9, with a much lower clinker content compared to W3 and W4 (W9 = 66%, W3 = 90%; W4 = 95%), shows a much lower Cl^- penetration depth. The effect of SCMs on the formation of Friedel's salt is mainly due to the influence on the formation of AFm phases which can also be affected by the use of aluminium sulphate accelerators [9]. Both, SCMs and the accelerator in the concrete mixture change the total Al_2O_3 contents, which correlate with the amount of CO_3-AFm formed for the mixtures W1–W8 ($R^2 = 0.72$; Supplement

Table 5 Calculated cement SP in comparison with the measured SP

Mixture	SP measured (kg/t)	Cement content [(%)	"Cement SP"(kg/t)
W1	0.66	100	0.66
W3	0.70	90	0.59
W6	0.34	60	0.39
W8	0.43	70	0.46
D10	0.69	100	0.69
D1b	0.55	80	0.55
D7	0.44	75	0.52
D8	0.50	70	0.48

Table 4). But neither the Al_2O_3 in the binder, nor the Friedel's salt formed seem to correlate linearly with the chloride diffusion coefficients for the eight mixtures analysed (W1–W8; respectively $R^2 = 0.29$; $R^2 = 0.23$). This may at least partially be related to the C–(A)–S–H formation and its binding capacity [80]. Additions, such as GGBFS, silica fume and metakaolin lead to higher C–(A)–S–H contents, especially with lower Ca/Si ratios, which are able to bind higher amounts of Na^{2+} ions and therefore the accompanying Cl^- [80]. Accordingly, not just the Friedel's salt but also the C–(A)–S–H content and composition may determine the Cl^- penetration resistance. In addition, porosity variations may be partly responsible for the lack of correlation between binding capacity and Cl^- diffusion coefficient [62]. Even though the total pore volume is similar for all 8 samples, ranging from 6.6 to 8.5%, the differences in the pore size distribution could have led to differences in chloride diffusion.

5.2 K_{ACC} vs K_{NAC}

Accelerated tests for concrete carbonation are often conducted to obtain data faster. However, the conversion of accelerated rates to natural rates does not always lead to successful results. Several conversion coefficients have been proposed in the literature, most of them based on specific experimental sets of samples, not always usable for slightly different mixtures or conditions [54, 55]. In particular, for shotcrete no data have been reported in the literature relating natural to accelerated carbonation rates. In the present study, the determined rates for natural and accelerated carbonation correlate linearly ($R^2 = 0.99$) (Fig. 9). To calculate the corresponding correction coefficient, the conversion approach from Hunkeler 2016 (Eq. 5; [55]) was modified by adjusting the correction factor (c). To calculate c a least square method was used resulting in ac value of 1.53. This c value is considerably higher than the one proposed by Hunkeler for conventional concrete, 1.19.

$$K_{N,ACC} = K_{ACC} \cdot \sqrt{\frac{[CO_{2\,atmosphere}]}{[CO_{2\,accelerated\,test}]}} \cdot c \qquad (5)$$
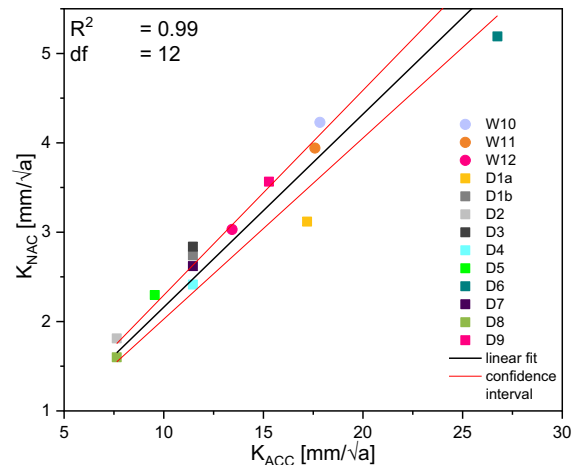

Fig. 9 Cross plot of natural carbonation rates against accelerated carbonation rates for the investigated shotcrete mixes. Note that the intercept point 0/0 was used for the correlation

5.3 Influence of shotcrete application

5.3.1 Wet- vs dry-mix

Dry-mix shotcrete showed higher sintering potential (SP 0.32–0.87 kg/t) and lower carbonation rates (0.4–0.9 mm/$\sqrt{d}$—excluding D6) compared to wet mix shotcrete (SP = 0.30–0.79 kg/t; K_{ACC} = 0.6–1.3 mm/$\sqrt{d}$) (Fig. 10). The CaO content in the various CEM I cements and the spray binder— CEM I, CEM I SR0-1, CEM I SR0-2, SPB—was very similar, $\sim$ 62–64%, and also the CaO in the binder of wet- and dry-mix samples showed no significant differences: 49–63% in dry-mix versus 51–64% in wet-mix shotcretes. Portlandite contents, however, differ considerably between dry- and wet-mix shotcrete: dry-mix samples contained more portlandite compared to wet-mix samples with similar mix design (Table 4; Fig. 10). This difference is hypothesized to be related to the higher calcium availability during the hydration process of dry-mix shotcrete. In the case of wet-mix shotcrete accelerated by means of aluminium sulphate, considerably high amounts of calcium are needed to form ettringite at the very early stages of hydration [9, 76]. In the case of dry-mix shotcretes produced with spray binder with low sulphate, lower quantities of calcium are expected to be needed for the formation of the AFm phases, responsible for the fast setting. In terms of pore size distribution, dry-mix shotcretes exhibited higher critical pore diameters and
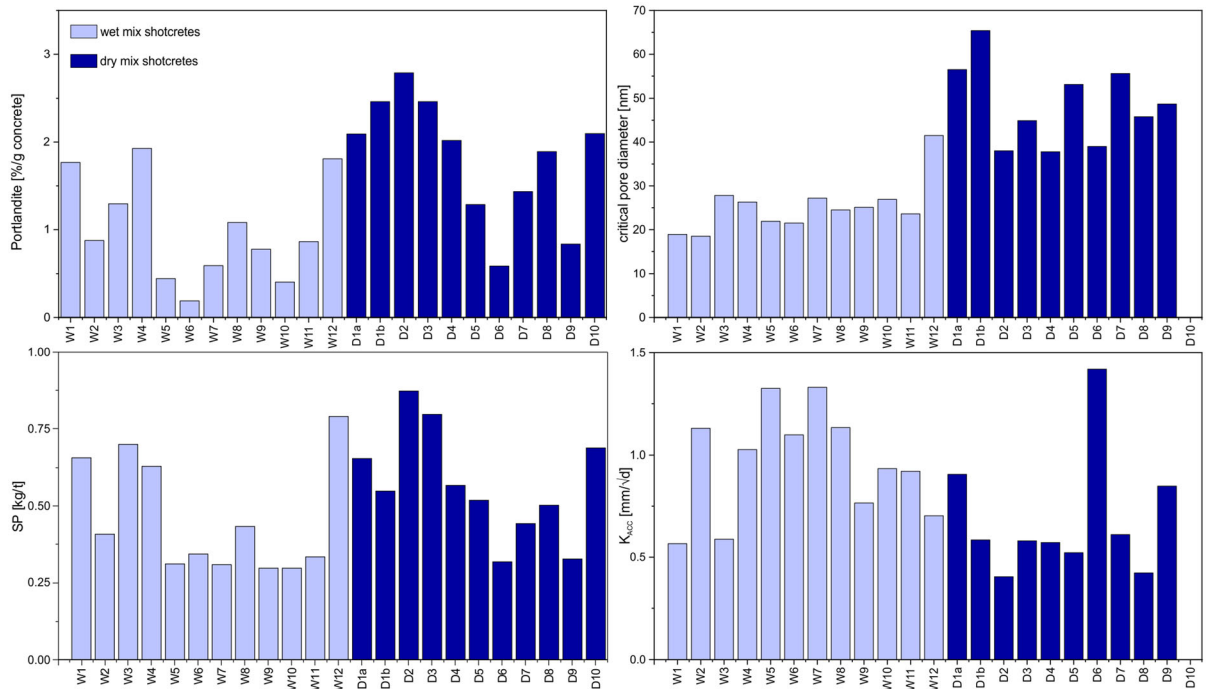
Fig. 10 Portlandite content, critical pore diameter, SP- and K_{ACC} values of wet- and dry-mix shotcretes showing differences between the two groups

broader pore size distribution than wet-mix samples (Fig. 10).

5.3.2 Influence of inhomogeneities/layers

The various durability tests carried out allowed for the characterisation of the durability of shotcrete mixes in terms of leaching, sintering, carbonation and chloride penetration, and for the correlation of performance distinct physical and chemical material characteristics. Moreover, inhomogeneities in the matrices attributed to the spraying process were observed in some occasions in the wet-mix samples. The layering, created presumably by the cyclic pumping of the concrete, in combination with the continuous dosing of the accelerator [15], resulted in regions (layers) with very low carbonation resistance compared to neighbouring 'high quality' areas. This fact raise an additional durability issue, which in turn affects all other durability parameters. Furthermore, the choice and extraction of specimens for shotcrete durability testing is at present influenced by this layering phenomenon: wrong conclusions may be drawn regarding the performance of shotcrete in terms of leaching or chloride penetration if the samples are not analysed systematically in various regions of, for example, a test panel. This is well illustrated by the very different Cl diffusion results obtained for sample W7 in the two samples analysed.

Improvements in the wet-mix spraying process would be necessary to prevent the formation of such heterogeneities and to produce high quality matrices. For example, the adjustment of the accelerator pumping process and dosage to the concrete pumping process and flow would be very beneficial.

Apart from the pulsating concrete versus continuous accelerator flow, the binder-rich peripheral zone and the enrichment in coarse aggregates in the centre of the spray jet may create other inhomogeneities in the matrices. This effect was reported by Ginouse and Jolin [13, 14], who observed the same pattern in the spray as in the receiving surface. Additionally, the rebound and the air trapped into the cement slurry can also lead to changes in the internal structure of the shotcrete and may cause macro and micro defects, as reported by Thomas [5].

Layering in dry-mix shotcrete was reported by Niu et al. 2015 [22]. They observed layering perpendicular to the spraying direction and corresponding lower resistance against sulphate attack in this weaker areas, which they attributed to higher porosity. In the present study no such layering was witnessed in dry-mix shotcrete, despite the higher rebound compared to wet-mix shotcrete and the fact that the water dosage was manually adjusted by the nozzle man. The lack of liquid accelerator and the lower flow rate used in the dry-mix process, 2.5 m^3/h, compared to the 12–20 m^3/h in the wet-mix spraying, together with the rotor-type dry-mix machine, instead of swing-tube piston pumping, probably allowed for a better distribution and homogeneity.

6 Conclusions

The durability of clinker reduced wet- and dry-mix shotcretes was assessed by investigating the resistance to leaching, carbonation and chloride penetration of real scale sprayed samples. The main conclusions drawn from this study are the following:

- Due to differences in hydration, the investigated dry-mix shotcretes formed more portlandite than the wet-mix shotcretes and therefore the Ca^{2+} leaching rates were higher, while carbonation rates were lower.
- Observed inhomogeneities/layering within the wet-mixes have the potential of significantly affecting the durability performance of the shotcrete, as exemplified by great variations in the carbonation depths of wet-mix shotcrete drill cores. We suggest that future optimizations of the spraying process and machine technology should focus on reducing the layering in the resulting material.
- Accelerated carbonation testing with 2 vol% CO_2 and 65% RH, led to the same trend in terms of carbonation rates as that observed within a sheltered natural carbonation test setup. The accelerated carbonation rates of the shotcrete mixtures can be converted to natural by using a correction factor of 1.53 and the square root of the CO_2 concentration ratio.

- Durability tests of clinker reduced shotcretes showed that the substitution of cement by SCMs:
  - o lowers the Ca^{2+} leaching due to dilution effects and portlandite consumption. Limestone as SCM should always be combined with pozzolanic or latent hydraulic SCMs to prevent higher Ca^{2+} leaching rates.
  - o enhances the carbonation rate due to the reduction of portlandite and the total reactive CaO in the system.
  - o have a positive effect on the chloride penetration resistance presumably due to changes on the microstructure and an increased binding effect.

In general, none of the proposed mixtures is optimized for all durability aspects. Reduced Ca^{2+} leaching and high carbonation resistance contradict each other due to the negative (SP) or positive (carbonation) effect of easily soluble Ca^{2+} bearing phases. High Al_2O_3 contents positively affect the chloride binding capacity through the formation of Friedel's salt, but can lead to a decreased sulphate resistance. Developing specifically optimized shotcrete mixes with different combinations of SCMs should be considered to meet the requirements of individual construction sites.

References

1. EFNARC (1996) European specification for sprayed concrete. EFNARC, Surrey

2. Hover KC (1997) Shotcrete for structural and architectural restoration of concrete shell built in 1905. Constr Build Mater 11:299–308. https://doi.org/10.1016/S0950-0618(97)00051-2

3. Bielak J, Hegger J (2018) Shell structures made of shotcrete with textile reinforcement—current development of design-, production- and testing methods (in German: Schalentragwerke aus Spritzbeton mit Textilbewehrung- aktuelle Entwicklungen bei Bemessungs-, Herstell- und Prüfm. In: Spritzbeton Tagung. pp 1–13

4. Kusterle W, Jäger J, John M, et al (2014) shotcrete in tunnel construction (in German: Spritzbeton im Tunnelbau). In: Bergmeister K, Fingerloos F, Wörner J-D (eds) 2014 Betonkalender Unterirdisches Bauen Grundbau

5. Thomas A (2009) Sprayed concrete lined tunnels: an introduction, 1. CRC Press, Boca Raton

6. Saade MRM, Passer A, Mittermayr F (2020) (Sprayed) concrete production in life cycle assessments: a systematic literature review. Int J Life Cycle Assess 25:188–207. https://doi.org/10.1007/s11367-019-01676-w

7. Saade MRM, Passer A, Mittermayr F (2018) A preliminary systematic investigation onto sprayed concrete's environmental performance. Procedia CIRP 69:212–217. https://doi.org/10.1016/j.procir.2017.11.108

8. Salvador RP, Cavalaro SHP, Segura I et al (2016) Early age hydration of cement pastes with alkaline and alkali-free accelerators for sprayed concrete. Constr Build Mater. https://doi.org/10.1016/j.conbuildmat.2016.02.101

9. Briendl LG, Mittermayr F, Baldermann A et al (2020) Early hydration of cementitious systems accelerated by aluminium sulphate: effect of fine limestone. Cem Concr Res. https://doi.org/10.1016/j.cemconres.2020.106069

10. Committee ACI (1995) Specification for shotcrete (ACI 506.2–95)

11. Jolin M, Burns D, Bissonnette B, et al (2009) Shotcrete for Underground support XI understanding the. In: Understanding the pumpability of concrete

12. Kaplan D, deLarrard F, Sedran T Design of concrete pumping circuit. ACI Mater J. https://doi.org/10.14359/14304

13. Ginouse N, Jolin M (2015) Investigation of spray pattern in shotcrete applications. Constr Build Mater 93:966–972. https://doi.org/10.1016/j.conbuildmat.2015.05.061

14. Ginouse N, Jolin M (2016) Mechanisms of placement in sprayed concrete. Tunn Undergr Sp Technol 58:177–185. https://doi.org/10.1016/j.tust.2016.05.005

15. Jolin M, Beaupre D (2004) Understanding wet-mix shotcrete; mix design, specifications and placement. Surf Support Min 263–267

16. Armelin HS, Banthia N (1998) Development of a general model of aggregate rebound for dry-mix shotcrete—(Part II). Mater Struct Constr 31:195–202. https://doi.org/10.1007/bf02480400

17. Armelin HS, Banthia N (1998) Mechanics of aggregate rebound in shotcrete - (Part I). Mater Struct Constr 31:91–98. https://doi.org/10.1007/bf02486470

18. Pan G, Li P, Chen L, Liu G (2019) A study of the effect of rheological properties of fresh concrete on shotcrete-rebound based on different additive components. Constr Build Mater 224:1069–1080. https://doi.org/10.1016/j.conbuildmat.2019.07.060

19. Galan I, Baldermann A, Kusterle W et al (2019) Durability of shotcrete for underground support–review and update. Constr Build Mater 202:465–493. https://doi.org/10.1016/j.conbuildmat.2018.12.151

20. Wang J, Niu D, Zhang Y (2015) Mechanical properties, permeability and durability of accelerated shotcrete. Constr Build Mater 95:312–328. https://doi.org/10.1016/j.conbuildmat.2015.07.148

21. Ma J (2011) Application of shotcrete linings under sulfate attack environments. Adv Mater Res 233–235:2061-2067. https://www.scientific.net/AMR.233-235.2061

22. Niu DT, De WY, Ma R et al (2015) Experiment study on the failure mechanism of dry-mix shotcrete under the combined actions of sulfate attack and drying-wetting cycles. Constr Build Mater 81:74–80. https://doi.org/10.1016/j.conbuildmat.2015.02.007

23. Mittermayr F, Baldermann A, Kurta C et al (2013) Evaporation—a key mechanism for the thaumasite form of sulfate attack. Cem Concr Res 49:55–64. https://doi.org/10.1016/J.CEMCONRES.2013.03.003

24. Steindl FR, Galan I, Baldermann A et al (2020) Cement and concrete research sulfate durability and leaching behaviour of dry- and wet-mix shotcrete mixes. Cem Concr Res. https://doi.org/10.1016/j.cemconres.2020.106180

25. Rinder T, Dietzel M, Leis A (2013) Calcium carbonate scaling under alkaline conditions - Case studies and hydrochemical modelling. Appl Geochem 35:132–141. https://doi.org/10.1016/j.apgeochem.2013.03.019

26. Dietzel M, Rinder T, Leis A et al (2008) Koralm tunnel as a case study for sinter formation in drainage systems—precipitation mechanisms and retaliatory action. Geomech und Tunnelbau 1:271–278. https://doi.org/10.1002/geot.200800024

27. Armengaud J, Cyr M, Casaux-Ginestet G, Husson B (2018) Durability of dry-mix shotcrete using supplementary cementitious materials. Constr Build Mater 190:1–12. https://doi.org/10.1016/j.conbuildmat.2018.09.107

28. Jolin M, Melo F, Bissonnette B, et al (2015) Evaluation of wet-mix shotcrete containing set-accelerator and service life prediction

29. Kaufmann JP (2014) Durability performance of fiber reinforced shotcrete in aggressive environment. WTC 2014 – Tunnels a better Life; 303:1–7

30. Lee S, Kim D, Ryu J et al (2006) An experimental study on the durability of high performance shotcrete for permanent tunnel support. Tunn Undergr Sp Technol 21:431. https://doi.org/10.1016/j.tust.2005.12.073

31. Park HG, Sung SK, Park CG, Won JP (2008) Influence of a C12A7 mineral-based accelerator on the strength and durability of shotcrete. Cem Concr Res 38:379–385. https://doi.org/10.1016/j.cemconres.2007.09.016

32. Won JP, Hwang UJ, Lee SJ (2015) Enhanced long-term strength and durability of shotcrete with high-strength C12A7 mineral-based accelerator. Cem Concr Res 76:121–129. https://doi.org/10.1016/j.cemconres.2015.05.020

33. Thumann M, Astner M, Saxer A, Kusterle W (2015) Precipitations in the tunnel drainage system—optimized shotcrete mix-design. Shotcrete undergr support XII

34. Salvador RP, Cavalaro SHP, Cano M, Figueiredo AD (2016) Influence of spraying on the early hydration of accelerated cement pastes. Cem Concr Res 89:187–199. https://doi.org/10.1016/j.cemconres.2016.07.015

35. Eichinger S, Boch R, Leis A et al (2020) Scale deposits in tunnel drainage systems—a study on fabrics and formation mechanisms. Sci Total Environ 718:1–22. https://doi.org/10.1016/j.scitotenv.2020.137140

36. Ulm FJ, Lemarchand E, Heukamp FH (2003) Elements of chemomechanics of calcium leaching of cement-based materials at different scales. Eng Fract Mech 70:871–889. https://doi.org/10.1016/S0013-7944(02)00155-8

37. Mainguy M, Tognazzi C, Torrenti JM, Adenot F (2000) Modelling of leaching in pure cement paste and mortar. Cem Concr Res 30:83–90. https://doi.org/10.1016/S0008-8846(99)00208-2

38. Baldermann C, Baldermann A, Furat O et al (2019) Mineralogical and microstructural response of hydrated cement blends to leaching. Constr Build Mater 229:1–15. https://doi.org/10.1016/j.conbuildmat.2019.116902

39. Pichler C, Saxer A, Lackner R (2012) Differential-scheme based dissolution/diffusion model for calcium leaching in cement-based materials accounting for mix design and binder composition. Cem Concr Res 42:686–699. https://doi.org/10.1016/j.cemconres.2012.02.007

40. Rosenqvist M, Bertron A, Fridh K, Hassanzadeh M (2017) Concrete alteration due to 55 years of exposure to river water: chemical and mineralogical characterisation. Cem Concr Res 92:110–120. https://doi.org/10.1016/j.cemconres.2016.11.012

41. Voegel C, Giroudon M, Bertron A et al (2019) Cementitious materials in biogas systems: biodeterioration mechanisms and kinetics in CEM I and CAC based materials. Cem Concr Res. https://doi.org/10.1016/j.cemconres.2019.105815

42. Dietzel M, Purgstaller B, Leis A et al (2013) Current challenges for scaling of tunnel drainage systems—modelling aproaches, monitoring tools and prevention strategies. Geomech und Tunnelbau 6:743–753. https://doi.org/10.1002/geot.201310014

43. Gamisch T, Girmscheid G (2007) Problematic of sintering in drainage systems of constructions (in German: Versinterungsprobleme in Bauwerksentwässerung), 1st edn. Bauwerk Verlag GmbH, Berlin

44. Austrian society for construction technology (2010) Guideline: tunnel drainage (in German: Tunnelentwässerung)

45. Girmscheid G, Gamisch T, Meinlschmidt A (2003) Sintering in tunnel drainages – recommendations for planning and building tunnels in supergene water (in German: Versinterung von Tunneldrainagen – Empfehlungen für die Planung und Bauausführung von Tunneln in deszendenten Wässern). Bauingenieur 78:478–487

46. Chen Y, Cui Y, Guimond Barrett A et al (2019) Investigation of calcite precipitation in the drainage system of railway tunnels. Tunn Undergr Sp Technol 84:45–55. https://doi.org/10.1016/j.tust.2018.10.021

47. De Weerdt K, Plusquellec G, Belda Revert A et al (2019) Effect of carbonation on the pore solution of mortar. Cem Concr Res 118:38–56. https://doi.org/10.1016/j.cemconres.2019.02.004

48. Galan I, Glasser FP (2014) Chloride in cement. Adv Cem Res 27:1–35. https://doi.org/10.1680/adcr.13.00067

49. Jovancicevic V, Bockris JOM, Carbajal JL, Zelenay P (1986) Adsorption and absorption of chloride ions on passive iron systems. J Electrochem Soc 133:2219–2226. https://doi.org/10.1149/1.2108377

50. Šavija B, Luković M (2016) Carbonation of cement paste: understanding, challenges, and opportunities. Constr Build Mater 117:285–301. https://doi.org/10.1016/j.conbuildmat.2016.04.138

51. Sevelsted TF, Skibsted J (2015) Carbonation of C–S–H and C–A–S–H samples studied by 13 C, 27 Al and 29 Si MAS NMR spectroscopy. Cem Concr Res 71:56–65

52. Shi Z, Lothenbach B, Geiker MR et al (2016) Experimental studies and thermodynamic modeling of the carbonation of Portland cement, metakaolin and limestone mortars. Cem Concr Res 88:60–72. https://doi.org/10.1016/j.cemconres.2016.06.006

53. Leemann A, Moro F (2017) Carbonation of concrete: the role of CO_2 concentration, relative humidity and CO_2 buffer capacity. Mater Struct Constr 50:1–14. https://doi.org/10.1617/s11527-016-0917-2

54. Van Den Heede P, De Schepper M, De Belie N (2019) Accelerated and natural carbonation of concrete with high volumes of fly ash: chemical, mineralogical and microstructural effects. R Soc Open Sci. https://doi.org/10.1098/rsos.181665

55. Hunkeler F (2012) Einfluss des CO2-Gehaltes, der Nach- und Vorbehandlung sowie der Luftfeuchtigkeit auf die Karbonatisierungsgeschwindigkeit von Beton (Influence of CO2-content, curing, preconditioning and relative humidity on the carbonation rate of concrete). Beton- und Stahlbetonbau 107:613–624. https://doi.org/10.1002/best.201200039

56. Galan I, Andrade C, Castellote M (2013) Natural and accelerated CO2 binding kinetics in cement paste at different relative humidities. Cem Concr Res 49:21–28. https://doi.org/10.1016/j.cemconres.2013.03.009

57. Sisomphon K, Franke L (2007) Carbonation rates of concretes containing high volume of pozzolanic materials. Cem Concr Res 37:1647–1653. https://doi.org/10.1016/j.cemconres.2007.08.014

58. Visser JHM (2012) Accelerated carbonation testing of mortar with supplementary cementing materials—limitation of the acceleration due to drying. Heron 57:231–247

59. Justnes H, Østvik J (2008) Effect of magnesium chloride as a dust binder on tunnel concrete paving

60. Hagelia P (2011) Sprayed concrete in aggressive subsea environment the Oslofjord test site. In: 6th int symp sprayed concr—mod use wet mix sprayed concr undergr support 15

61. Bothe JV, Brown PW (2004) PhreeqC modeling of Friedel's salt equilibria at 23 ± 1 °C. Cem Concr Res 34:1057–1063. https://doi.org/10.1016/j.cemconres.2003.11.016

62. Loser R, Lothenbach B, Leemann A, Tuchschmid M (2010) Chloride resistance of concrete and its binding capacity—comparison between experimental results and

thermodynamic modeling. Cem Concr Compos 32:34–42. https://doi.org/10.1016/j.cemconcomp.2009.08.001

63. Chang H (2017) Chloride binding capacity of pastes influenced by carbonation under three conditions. Cem Concr Compos 84:1–9. https://doi.org/10.1016/j.cemconcomp.2017.08.011

64. De Weerdt K, Colombo A, Coppola L, Justnes H, Geiker MR (2015) Impact of the associated cation on chloride binding of Portland cement paste. Cem Concr Res 68:196–202

65. Kayali O, Khan MSH, Sharfuddin Ahmed M (2012) The role of hydrotalcite in chloride binding and corrosion protection in concretes with ground granulated blast furnace slag. Cem Concr Compos 34:936–945. https://doi.org/10.1016/j.cemconcomp.2012.04.009

66. Beaudoin JJ, Ramachandran VS, Feldman RF (1990) Interaction of chloride and C-S-H. Cem Concr Res 20:875–883

67. European Committee for Standardization (2015) EN 12390–11 Testing hardened concrete—part 11: determination of the chloride resistance of concrete, unidirectional diffusion

68. Nordtest Build 443 (1995) Concrete, hardened: accelerated chloride penetration. NT BUILD 443

69. Delagrave A, Marchand J, Ollivier JP et al (1997) Chloride binding capacity of various hydrated cement paste systems. Adv Cem Based Mater 6:28–35. https://doi.org/10.1016/S1065-7355(97)00007-2

70. Tang L, Nilsson L-O (1993) Chloride binding capacity and binding isotherms of opc pastes and mortars. Cem Concr Res 23:247–253

71. Lothenbach B, Scrivener K, Hooton RD (2011) Supplementary cementitious materials. Cem Concr Res 41:1244–1256. https://doi.org/10.1016/j.cemconres.2010.12.001

72. Juhart J, David GA, Saade MRM et al (2019) Functional and environmental performance optimization of Portland cement-based materials by combined mineral fillers. Cem Concr Res 122:157–178. https://doi.org/10.1016/j.cemconres.2019.05.001

73. Salvador RP, Rambo DAS, Bueno RM et al (2019) On the use of blast-furnace slag in sprayed concrete applications. Constr Build Mater 218:543–555. https://doi.org/10.1016/j.conbuildmat.2019.05.132

74. Galan I, Briendl L, Thumann M et al (2019) Filler Effect in Shotcrete. Materials 12:1–24. https://doi.org/10.3390/ma12193221

75. Lothenbach B, Le Saout G, Gallucci E, Scrivener K (2008) Influence of limestone on the hydration of Portland cements. Cem Concr Res 38:848–860. https://doi.org/10.1016/j.cemconres.2008.01.002

76. Salvador RP, Cavalaro SHP, Cincotto MA, Figueiredo AD (2016) Parameters controlling early age hydration of cement pastes containing accelerators for sprayed concrete. Cem Concr Res 89:230–248. https://doi.org/10.1016/j.cemconres.2016.09.002

77. Gaitero JJ, Campillo I, Guerrero A (2008) Reduction of the calcium leaching rate of cement paste by addition of silica nanoparticles. Cem Concr Res 38:1112–1118. https://doi.org/10.1016/j.cemconres.2008.03.021

78. Choi P, Yun KK, Yeon JH (2017) Effects of mineral admixtures and steel fiber on rheology, strength, and chloride ion penetration resistance characteristics of wet-mix shotcrete mixtures containing crushed aggregates. Constr Build Mater 142:376–384. https://doi.org/10.1016/j.conbuildmat.2017.03.093

79. Shi Z, Geiker MR, Lothenbach B et al (2017) Friedel's salt profiles from thermogravimetric analysis and thermodynamic modelling of Portland cement-based mortars exposed to sodium chloride solution. Cem Concr Compos 78:73–83. https://doi.org/10.1016/j.cemconcomp.2017.01.002

80. Papadakis VG (2000) Effect of supplementary cementing materials on concrete resistance against carbonation and chloride ingress. Cem Concr Res 30:291–299

81. Austrian standards institute (2011) ÖNORM EN 197–1 Part 1: composition, specifications and conformity criteria for common cements

82. Austrian standard institute (2010) ÖNORM B 3309–1 Processed hydraulic additions for concrete production—part 1: combination products

83. Austrian society for construction technology (2009) Guidline: sprayed concrete (in German: Richtlinie Spritzbeton)

84. Austrian society for construction technology (2012) sintering potential determination (in German: Festlegung des Reduzierten Versinterungspotenials)

85. Austrian standards institute (2010) ONR CEN/TS 12390–12 Testing hardened concrete—part 12: determination of the carbonation resistance of concrete—accelerated carbonation method

86. fib Task Group 5.6 (2006) Model Code für Service Life Desing. In: Concrete IF for S (ed) fib Bulletin. Sprint Digital Druck, Stuttgart

87. Birnin-Yauri UA, Glasser FP (1998) Friedel's salt, $Ca_2Al(OH)_6(Cl, OH) \cdot 2H_2O$: its solid solutions and their role in chloride binding. Cem Concr Res 28:1713–1723. https://doi.org/10.1016/S0008-8846(98)00162-8

88. Shah V, Scrivener K, Bhattacharjee B, Bishnoi S (2018) Changes in microstructure characteristics of cement paste on carbonation. Cem Concr Res 109:184–197. https://doi.org/10.1016/j.cemconres.2018.04.016

89. Leemann A, Nygaard P, Kaufmann J, Loser R (2015) Relation between carbonation resistance, mix design and exposure of mortar and concrete. Cem Concr Compos 62:33–43. https://doi.org/10.1016/j.cemconcomp.2015.04.020